

Synthesis of III-N_x-V_{1-x} Thin Films by N Ion Implantation

K. M. Yu, W. Walukiewicz, W. Shan¹, J. Wu, J. W. Beeman, J. W. Ager III, E. E. Haller, and M. C. Ridgway²

Materials Sciences Division, Lawrence Berkeley National Laboratory,
Berkeley, California 94720;

¹ OptiWork, Inc. Fremont, CA 94538

² Department of Electronic Materials Engineering, Research School of Physical Sciences and Engineering, Australian National University, Canberra, Australia

ABSTRACT

Dilute III-N_x-V_{1-x} alloys were successfully synthesized by nitrogen implantation in GaAs and InP. The fundamental band gap energy for the ion beam synthesized III-N_x-V_{1-x} alloys was found to decrease with increasing N implantation dose in a manner similar to that commonly observed in epitaxially grown GaN_xAs_{1-x} and InN_xP_{1-x} thin films. The fraction of N occupying anion sites ("active" N) in the GaN_xAs_{1-x} layers formed by N implantation was thermally unstable and decreased with increasing annealing temperature. In contrast, thermally stable InN_xP_{1-x} alloys with N mole fraction as high as 0.012 were synthesized by N implantation in InP. Moreover, the N activation efficiency in InP was at least a factor of two higher than in GaAs under similar processing conditions. The low N activation efficiency (<20%) in GaAs can be improved by co-implanting Ga and N in GaAs.

INTRODUCTION

It is now well established that incorporation of small amounts of nitrogen into GaAs to form dilute GaN_xAs_{1-x} alloys has a profound effect on the fundamental band gap [1-6]. Reduction of the band gap by more than 100 meV per atomic percent of N was first observed in GaN_xAs_{1-x} alloys grown by plasma-assisted metalorganic chemical vapor deposition [2,3]. A similar gap reduction was observed also in other III-N_x-V_{1-x} semiconductor alloys [2-4,6-8]. The strong dependence of the band gap as well as the lattice constant on the N content has made these N containing III-V alloys potentially important materials for long wavelength optoelectronic devices [9,10] and high efficiency hybrid solar cell applications [11,12]

There were several theoretical studies aimed at explaining the unusually strong dependence of the fundamental gap on the N content in the GaN_xAs_{1-x} alloys [13-16]. Recently, Shan *et al.* [17] have shown that an anticrossing interaction between the narrow band of localized N states and the extended conduction band states of the host semiconductor matrix gives rise to a splitting of the conduction band into two non-parabolic subbands in GaN_xAs_{1-x} alloys [17,18]. According to this band anticrossing model, the dispersion relations for the upper and lower conduction subbands in GaN_xAs_{1-x} are given by [18]:

$$E_{\pm}(k) = \frac{1}{2} \left[E_N + E_M(k) \pm \sqrt{(E_N - E_M(k))^2 + 4C_{NM}^2 x} \right] \quad (1)$$

where E_N is the energy of the N level, $E_M(k)$ is the standard parabolic dispersion relation for the host semiconductor matrix, and C_{NM} is the matrix element describing the coupling between N-

Table I. Detailed information on the N implantation conditions on the various samples.

Implant	Implanted N (%)	Energy (keV)	Dose (at./cm ²)	Total dose (at./cm ²)
N (single implant)	0.8	160	4×10^{15}	6.63×10^{15}
		77	1.7×10^{15}	
		35	9.3×10^{14}	
	1.6	160	8×10^{15}	1.326×10^{16}
		77	3.4×10^{15}	
		35	1.86×10^{15}	
	1.8	120	6.3×10^{15}	9.5×10^{15}
		60	2.4×10^{15}	
		35	8.0×10^{14}	
	2.0	100	7.0×10^{15}	1.03×10^{16}
		50	2.5×10^{15}	
		33	8.0×10^{14}	
	3.6	120	1.26×10^{16}	1.7×10^{16}
		60	4.8×10^{15}	
		35	1.6×10^{15}	
	1.6	160	2.4×10^{16}	3.98×10^{16}
		77	1.02×10^{16}	
		35	5.58×10^{15}	
N (co-implant)	2.0	450	1.5×10^{16}	2.15×10^{16}
		255	6.5×10^{15}	
Ga (co-implant)	2.0	1250	2.4×10^{16}	2.4×10^{16}

states and the extended states. For $\text{GaN}_x\text{As}_{1-x}$, the downward shift of the lower subband E_c can account well for the reduction of the fundamental band gap using the known values of $E_N=1.65$ eV above the valence band maximum and $C_{NM}=2.7$ eV [17,18].

Since only a small amount of N (<1%) can lead to a large reduction in the energy band gap of III-N-V materials, ion implantation is an attractive and feasible approach to synthesize III-N_x-V_{1-x} alloys. In this paper we report a study of the optical properties of $\text{GaN}_x\text{As}_{1-x}$ and $\text{InN}_x\text{P}_{1-x}$ alloy thin films formed by N ion implantation.

EXPERIMENTAL DETAILS

Nitrogen ions were implanted into semi-insulating GaAs and InP. Multiple energy N-implantations were chosen to form ~2000-3500 Å thick layers with uniform N atomic concentration. Several N doses were used to create dilute nitride layers with different implanted N mole fraction, $x_{imp} \approx 0.8, 1.6, 1.8, 2, 3.6, 4.8\%$. It is important to recognize that only a limited fraction of all the implanted N will occupy proper sublattice sites (i.e. get "activated") after annealing. All implantations were carried out using a beam current of ~0.2-0.5 μA/cm². The details of the implantation are tabulated in Table I. For the Ga+N co-implanted GaAs samples a 3000 Å thick SiO₂ layer was deposited on the GaAs substrate before implantation. Rapid thermal annealing (RTA) was carried out on the implanted samples in a flowing N₂ ambient in the

temperature range of 560-950°C for 5-120 seconds with the sample surface protected by either a blank GaAs or InP wafer.

The band gap energy of the samples was examined by Photomodulated Reflectance (PR) measurements at room temperature. Quasi-monochromatic light from a 300 W halogen tungsten lamp dispersed by a 0.5 m monochromator was focused on the samples as a probe beam with beam size ~1mm. A HeCd laser beam (4420 Å) chopped at 260 Hz provided the modulation. PR signals were detected by a Ge or Si photodiode using a phase-sensitive lock-in amplification system. The spectral resolution of the system at the GaAs band gap is <3meV.

RESULTS AND DISCUSSION

Fig. 1 shows a series of PR spectra from an unimplanted and N-implanted GaAs samples with $x_{imp} \approx 1.8, 2$ and 3.6% after RTA at 800°C for 10 sec. The PR spectra shown in Fig. 1 exhibit well-resolved spectral features related to the interband transitions. The significant broadening of the features in the implanted samples can be attributed to the implantation damage. The downward energy shift increases with implantation dose, similar to the band gap energy reduction observed in GaN_xAs_{1-x} alloys with increasing N content [2-6]. The possibility of band-gap reduction (ΔE) due to lattice damage created by the implantation was also investigated. PR measurements on a 200 keV Ga-implanted sample showed a considerable broadening of the PR features but no noticeable shift of the PR transition energies [6]. These observations indicate that although the lattice damage broadens the spectral features associated with interband transitions the band gap reduction in the N-implanted GaAs samples is a direct result of the formation of GaN_xAs_{1-x} alloy layers.

The "active" N contents (N incorporated on the As sublattice) in the ion beam

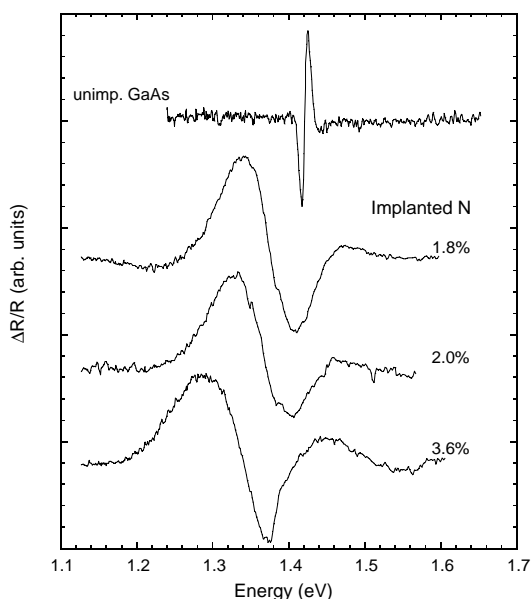


Figure 1. A series of PR spectra from N implanted GaAs with implanted doses corresponding to N mole fractions of 1.8, 2 and 3.6% after 10sec RTA at 800°C.

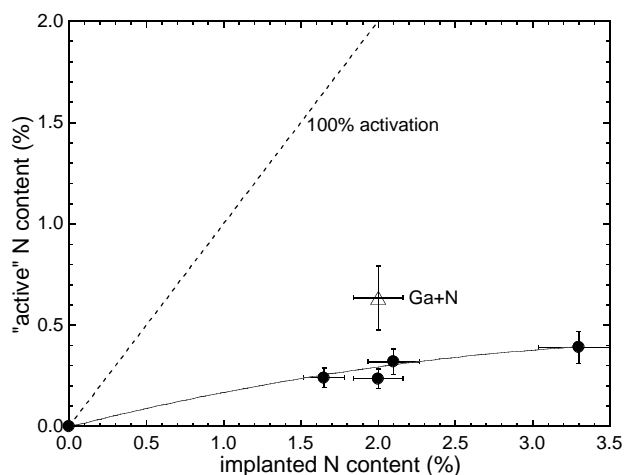


Figure 2. Amount of N incorporated in the N implanted GaAs samples with different implanted N dose after RTA at 800°C 10sec. The amount of active N was calculated from the band gap reduction as observed from Figure 1 using Equation (1).

synthesized $\text{GaN}_x\text{As}_{1-x}$ layers were derived from the observed ΔE using Eq. (1). The results are shown in Fig. 2. It is seen from this figure that only a small fraction ($<15\%$) of the implanted N is "active" in the GaAs samples after RTA at 800°C for 10 sec. The low N activation efficiency was enhanced by more than a factor of two when an equal amount of Ga atoms was co-implanted with N in GaAs. This is apparently due to the creation of a locally non-stoichiometric (Ga-rich) region with a high concentration of As vacancies available for N substitution. With Ga co-implantation, an "active" N content of 0.65% has been achieved with a x_{imp} of only 1.8%. Without Ga co-implantation, the highest "active" N content of 0.4% has been achieved by implantation of 3.3% N into GaAs. Also, a large decrease in ΔE was observed as the RTA temperature was increased. In fact, only a negligible band gap reduction ΔE (~ 10 meV) was observed when the RTA temperature exceeded 900°C , indicating that less than 0.1% of N remained substitutional in the As sublattice.

The optical transitions from $\text{InN}_x\text{P}_{1-x}$ formed by N-implantation into InP and RTA at 800°C for 10sec are shown in Fig. 3. Similar to the case of N implanted GaAs, a monotonic decrease in the band gap is observed as the implanted N dose increases. For the highest N dose of 4.8%, the band gap is estimated to be 1.17eV, corresponding to $\Delta E=180$ meV. Figure 4 shows the dependence of the $\text{InN}_x\text{P}_{1-x}$ band gap on the N mole fraction for epitaxially grown thin films. The absorption data in the figure are from the original Bi and Tu study [4] and the PR data were obtained by Shan *et al.* from similar $\text{InN}_x\text{P}_{1-x}$ thin films [19]. The solid line in Fig. 4 is the edge of the lower subband E. calculated from the band anticrossing model (Eq. (1)), using $E_M=1.35$ eV for the InP matrix. The energy of the highly localized N level $E_N=2.0$ eV relative to the valence band edge in InP was estimated from the valence band offset

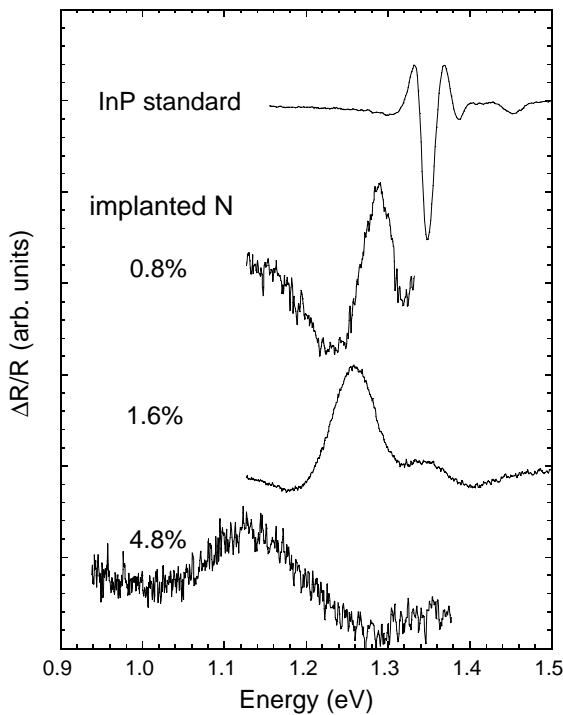


Figure 3. The PR spectra from N implanted InP with x_{imp} of 0.008, 0.016 and 0.048 after 10sec RTA at 800°C .

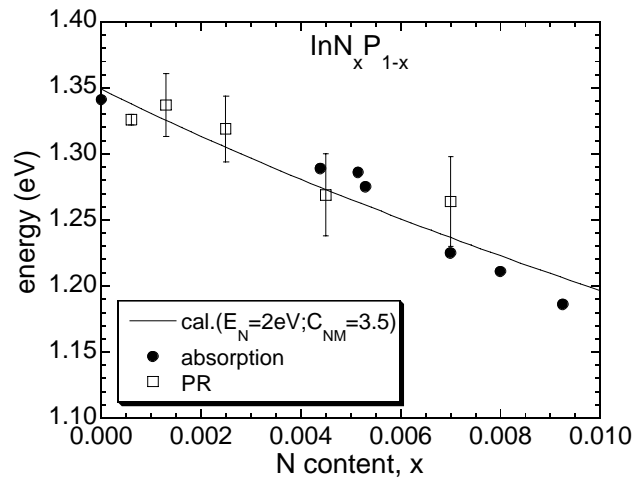


Figure 4. Band gap energy as a function of N content in $\text{InN}_x\text{P}_{1-x}$ alloy thin films grown by GSMBE. The solid line is the calculated dependence of the E. edge on x according to the band anticrossing model using the known band structure parameters of InP.

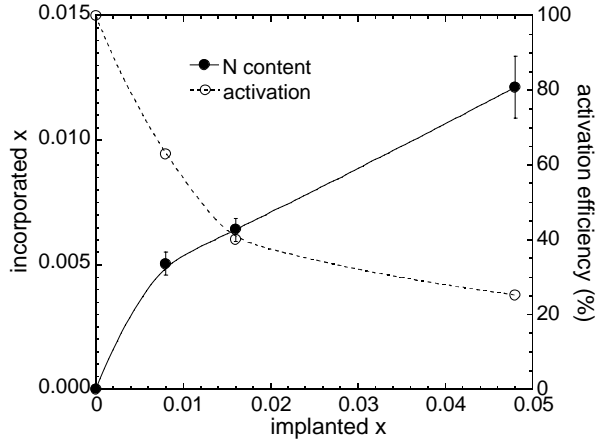


Figure 5. The "active" N incorporated in the P sublattice calculated from the band gap reduction using the band anticrossing model plotted as a function of implanted N. The activation efficiency of N in the three cases is also plotted.

Moreover, only a small decrease in ΔE ($<20\text{meV}$) is observed over the annealing range used in this study, indicating that the N incorporated in the P sublattice are thermally stable to at least 850°C . This is in contrast to $\text{GaN}_x\text{As}_{1-x}$ layers synthesized by N implantation in GaAs. For these alloys we found that the configuration with N atoms substituting As sites is thermally much less stable.

The high activation efficiency and the good thermal stability of N in InP may be due to the small difference between the bond energy of In-N (5.77 eV) and In-P (5.81 eV). In contrast, in the Ga-N-As system the Ga-N bond (6.81 eV) is much stronger than that of the Ga-As (5.55 eV). Therefore it may be energetically more favorable for the N atoms to "deactivate" by forming GaN clusters during annealing. The smaller size difference between the N and P atoms compared to that between the N and As atoms may also contribute to the improved substitution of N in the P sublattice.

In addition to the lower subband E_- that is responsible to the reduction in the fundamental band gap in $\text{III-N}_x\text{-V}_{1-x}$ alloys, the band anticrossing model also predicts the formation of an upper subband E_+ (Equation (1)). The PR spectrum on N implanted InP sample with $x_{\text{imp}} \approx 0.016$ after RTA at 800°C for 10sec taken over a wide photon energy range (1.1-2.3 eV) reveals a new PR feature corresponding to the transition associated with the E_+ edge at 2.1 eV. This transition corresponds to an energy shift from the localized N states $E_+ - E_N = 100\text{meV}$, in perfect agreement with the downward energy shift $E_M - E_- = 100\text{meV}$ for this sample. This again confirms that the band anticrossing model provides a quantitative description for the N induced modifications in the conduction band of the $\text{III-N}_x\text{-V}_{1-x}$ alloy system.

CONCLUSION

We have successfully synthesized dilute $\text{III-N}_x\text{-V}_{1-x}$ alloys (with $x=0.002\text{-}0.012$) by N

$\Delta E(\text{GaAs/InP})=0.35\text{ eV}$. We found that the experimental data in Fig. 4 are best described with a coupling matrix element $C_{\text{NM}}=3.5\text{ eV}$.

Using this fitted parameter, we calculated the N content in $\text{InN}_x\text{P}_{1-x}$ layers synthesized by N implantation from the ΔE values; the results are presented in Fig. 5. The amounts of N incorporated in the P sublattice in the $\text{InN}_x\text{P}_{1-x}$ layers were $x=0.005$, 0.0065 and 0.012 for samples with $x_{\text{imp}} \approx 0.008$, 0.016 and 0.048 , respectively. Notice that the maximum x value achieved, 0.012 , exceeds that reported to date ($x=0.009$) [4] for epitaxially grown $\text{InN}_x\text{P}_{1-x}$ thin films.

It is also important to note in Fig. 5 that the activation efficiency of N in InP decreases as x_{imp} increases. This may be the sign for a limited solubility of N in the InP matrix. For N implantation doses in the x_{imp} range of $0.01\text{-}0.02$, the activation efficiency is $\sim 35\text{-}45\%$, over a factor of 2 higher than that in N- implanted GaAs.

implantation in GaAs and InP. Band gap reductions in the range of 60-180meV were achieved in these ion synthesized $\text{III-N}_x\text{-V}_{1-x}$ alloys. The band gap reduction can be explained by the anticrossing interaction between the narrow band of localized N states and the extended conduction band states of the host semiconductor matrix. $\text{InN}_x\text{P}_{1-x}$ with N contents x as high as 0.012 was synthesized. Both the N activation efficiency and thermal stability of ion synthesized $\text{InN}_x\text{P}_{1-x}$ alloys were found to be higher than those for N implanted GaAs under similar processing conditions.

ACKNOWLEDGMENT

This work was supported by the "Photovoltaic Materials Focus Area" in the DOE Center of Excellence for the Synthesis and Processing of Advanced Materials, Office of Science, Office of Basic Energy Sciences, Division of Materials Sciences under U.S. Department of Energy Contract No. DE-ACO3-76SF00098.

REFERENCES

1. M. Weyers, M. Sato, H. Ando, *Jpn. J. Appl. Phys.* **31**, L853 (1992).
2. J. N. Baillargeon, K. Y. Cheng, G. F. Hofler, P. J. Pearah and K. C. Hsieh, *Appl. Phys. Lett.* **60**, 2540 (1992).
3. M. Kondow, K. Uomi, K. Hosomi and T. Mozume, *Jpn. J. Appl. Phys.* **33** L1056 (1994).
4. W. G. Bi, and C. W. Tu, *J. Appl. Phys.* **80**, 1934 (1996).
5. K. Uesugi, N. Marooka and I. Suemune, *Appl. Phys. Lett.* **74**, 1254 (1999).
6. W. Shan, K. M. Yu, W. Walukiewicz, J. W. Ager, E. E. Haller and M. C. Ridgway, *Appl. Phys. Lett.* **75**, 1410 (1999).
7. W. G. Bi and C. W. Tu, *Appl. Phys. Lett.* **69**, 3710 (1996).
8. X. P. Xin and C. W. Tu, *Appl. Phys. Lett.* **72**, 2442 (1998).
9. M. Kondow, T. Kitatani, S. Nakatsuka, M. C. Larson, K. Nakahara, Y. Yazawa, M. Okai and K. Uomi, *IEEE J. Sel. Topics in Quantem Elect.* **3**, 719 (1997).
10. M. Kondow, T. Kitatani, M. C. Larson, K. Nakahara, K. Uomi and H. Inoue, *J. Crystal Growth* **188**, 255 (1998).
11. D. J. Friedman, J. F. Geisz, S. R. Kurtz, D. Myers and J. M. Olson, *J. Cryst. Growth* **195**, 409 (1998).
12. S. R. Kurtz, A.A. Allerman, E.D. Jones, J.M. Gee, J.J. Banas, and B.E. Hammons, *Appl. Phys. Lett.* **74**, 729(1999).
13. J. Neugebauer and C. G. Van Walle, *Phys. Rev.* **B51**, 10568 (1995).
14. L. -W. Wang, L. Bellaiche, S. -H. Wei, and A. Zunger, *Phys. Rev. Lett.* **80**, 4725 (1998).
15. E. D. Jones, N. A. Modine, A. A. Allerman, S. R. Kurtz, A. F. Wright, S. T. Tozer, and X. Wei, *Phys. Rev.* **B60**, 4430 (1999).
16. A. Lindsay and E. P. O'Reilly, *Solid State Commun.* **112**, 443 (1999).
17. W. Shan, W. Walukiewicz, J. W. Ager III, E. E. Haller, J. F. Geisz, D. J. Friedman, J. M. Olson, and S. R. Kurtz, *Phys. Rev. Lett.* **82**, 1221(1999).
18. W. Walukiewicz, W. Shan, J. W. Ager III, D. R. Chamberlin, E. E. Haller, J. F. Geisz, D. J. Friedman, J. M. Olson, and S. R. Kurtz, in *Photovoltaics for the 21st Century*, edited by V. K. Kapur, R. D. McDonnell, D. Carlson, G. P. Ceasar, A. Rohatgi (Electrochemical Society Press, Pennington, 1999) p. 190.
19. W. Shan, K. M. Yu, W. Walukiewicz, X. P. Xin, and C. W. Tu, unpublished data (2000).